

This is the peer reviewed version of the following article:

Assessing feature relevance in NPLS models by VIP / Favilla, Stefania; Durante, Caterina; LI VIGNI, Mario; Cocchi, Marina. - In: CHEMOMETRICS AND INTELLIGENT LABORATORY SYSTEMS. - ISSN 0169-7439. - STAMPA. - 129:(2013), pp. 76-86. [10.1016/j.chemolab.2013.05.013]

*Terms of use:*

The terms and conditions for the reuse of this version of the manuscript are specified in the publishing policy. For all terms of use and more information see the publisher's website.

20/04/2024 17:50

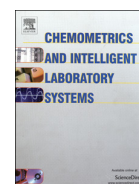
(Article begins on next page)



ELSEVIER

Contents lists available at SciVerse ScienceDirect

## Chemometrics and Intelligent Laboratory Systems

journal homepage: [www.elsevier.com/locate/chemolab](http://www.elsevier.com/locate/chemolab)

## Q41 Assessing feature relevance in NPLS models by VIP

Q1Q2 2 Stefania Favilla<sup>a</sup>, Caterina Durante<sup>b</sup>, Mario Li Vigni<sup>b</sup>, Marina Cocchi<sup>b,\*</sup>3 <sup>a</sup> Department of Biomedical Sciences, Metabolic and Neuroscience, University of Modena and Reggio Emilia, Italy4 <sup>b</sup> Department of Chemical and Geological Sciences, University of Modena and Reggio Emilia, Italy

## ARTICLE INFO

## 6 Article history:

7 Received 9 January 2013

8 Received in revised form 17 April 2013

9 Accepted 26 May 2013

10 Available online xxxx

## 11 Keywords:

12 VIP

13 Multi-way data

14 NPLS

15 NPLS-DA

16 Feature selection

## ABSTRACT

Multilinear PLS (NPLS) and its discriminant version (NPLS-DA) are very diffuse tools to model multi-way data arrays. Analysis of NPLS weights and NPLS regression coefficients allows data patterns, feature correlation and covariance structure to be depicted. In this study we propose an extension of the Variable Importance in Projection (VIP) parameter to multi-way arrays in order to highlight the most relevant features to predict the studied dependent properties either for interpretative purposes or to operate feature selection. The VIPs are implemented for each mode of the data array and in the case of multivariate dependent responses considering both the cases of expressing VIP with respect to each single y-variable and of taking into account all y-variables altogether.

Three different applications to real data are presented: i) NPLS has been used to model the properties of bread loaves from near infrared spectra of dough, acquired at different leavening times, and corresponding to different flour formulations. VIP values were used to assess the spectral regions mainly involved in determining flour performance; ii) assessing the authenticity of extra virgin olive oils by NPLS-DA elaboration of gas chromatography/mass spectrometry data (GC–MS). VIP values were used to assess both GC and MS discriminant features; iii) NPLS analysis of a fMRI-BOLD experiment based on a pain paradigm of acute prolonged pain in healthy volunteers, in order to reproduce efficiently the corresponding psychophysical pain profiles. VIP values were used to identify the brain regions mainly involved in determining the pain intensity profile.

© 2013 Published by Elsevier B.V.

## 1. Introduction

Multilinear PLS (NPLS) and its discriminant version (NPLS-DA) are very diffuse tools to model multi-way data arrays. NPLS represents the multi-way extension of two-way partial least squares regression (PLS) for multi-way data and was first developed by Bro in 1996 [1] and successively by Bro, Smilde and De Jong [2–4].

It has been demonstrated that multi-way data analysis tools, taking into account the multi-way structure of data are much more efficient compared to unfolding procedures, that is re-arranging the multi-way data into a two-way matrix structure and then applying bilinear models. Multi-way analysis allows simplifying the interpretation of the results and providing more adequate and robust models using relatively few parameters [5,6]. While this is true in general, it is worth noticing that when dealing with real-time monitoring, e.g. in batch process monitoring, N-way models may not represent a real advantage with respect to adopting a proper unfolding/refolding procedure as by using Multiway-PCA [7].

In particular, the use of NPLS shares all the advantages of latent variable based regression and discrimination methods, from the point of view of data visualization and interpretation [8–10]. In fact, analysis of

NPLS weights and NPLS regression coefficients allows data patterns, feature correlation and covariance structure to be depicted.

However, it is often needed to define which are the most relevant features to predict the studied dependent properties either for interpretative purposes, e.g. to provide a better understanding of the underlying process that generated the data, or to operate feature selection in order to reduce the noise generated by irrelevant features or to reduce data redundancy.

Some of the several variable selection methods applied to two-way data matrices in the context of PLS regression [11], such as interval PLS (iPLS) [12] or genetic algorithms [13], can be as well suited for NPLS if the X-block multi-way data array has only one spectral dimension, e.g. samples × spectral profiles × time [14]. When the data array has two spectral dimensions, or more generally when a two-dimensional signal map characterizes each sample, as generated by hyphenated analytical techniques, such as emission/excitation fluorescence, chromatography/mass spectrometry, etc., these variable selection methodologies present significant challenges and it is suggested to apply them after unfolding the data array [15]. However, in this way, the multi-way data structure is not taken into account in the variable selection step, thus losing the multi-way analysis advantage.

Moreover, a general distinction can be made among tools, which accomplish feature selection by deleting a set of features and re-assessing the performance of the reduced models, thus requiring extensive model

\* Corresponding author. Tel.: +39 059 2055029; fax: +39 059 373543.  
E-mail address: [marina.cocchi@unimore.it](mailto:marina.cocchi@unimore.it) (M. Cocchi).

validation, and those that operate a ranking of the features according to their relevance. Concerning the latter type, congruence loadings [16], VIP (Variable Importance in Projection) [17–20], and selectivity ratio [21] have gained increasing attention as an important measure of each explanatory variable or predictor.

The aim of this work is to extend the VIP method to multi-way arrays and to develop accompanying code. A similar attempt has been reported previously [22] but our formulation is, in our opinion, more straightforward and closer to VIP definition for two-way data. In fact, the VIP definition given in Ref. [22] does not reproduce the two-way VIP formulation, which consists, for each X-variable, of a sum, over latent variables, of its PLS-weight weighted by the percentage of explained Y variance. The reason is due to the fact that the NPLS mode 1 scores for X-block (T), which are linked to Y by the NPLS inner-relation, are substituted by a different projection of unfolded-X through NPLS weights. Usually, in the case of several dependent responses (multivariate Y) VIP is defined taking into account all y-variables altogether. Here we consider as well, the possibility of expressing VIP with respect to each single y-variable (this is a further difference with the approach presented in Ref. [22] that does not allow this possibility). This offers higher flexibility to the method and can be particularly useful to interpret discriminant NPLS-DA models, since the VIP for single y-variables corresponds, in this case, to the most discriminant feature for each category. However, it is beyond the aim of this paper, to compare the use of VIPs with other feature selection methodologies for multi-way arrays, actually in the applications presented here variable selection is not operated and VIPs are used more on an interpretative ground.

## 2. Methods

### 2.1. Multilinear partial least squares (NPLS)

Multilinear PLS (NPLS) represents the extension of two-way partial least squares regression (PLS) to data arrays of any order considering both X and Y-blocks. In the following, the method is described considering the case of a three-way data array,  $\mathbf{X}$ , but the extension to further dimensions can be simply deduced. As for the dependent variables Y-block, we will describe here the case of a two-way matrix, but the method can be easily extended to higher orders in the Y-block [1].

Specifically, PLS regression aims to find a relationship between a set of predictor (independent) data,  $\mathbf{X}$ , and a set of responses (dependent),  $\mathbf{Y}$ . In the more general case, the arrays of independent,  $\mathbf{X}$  and dependent  $\mathbf{Y}$  variables are decomposed in such a way that the score vectors from these models have pair-wise maximal covariance [3,4]. Multilinear PLS was firstly developed as a PARAFAC-like model of  $\mathbf{X}$  and it was shown that the method could be easily extended to any desired order for both  $\mathbf{X}$  and  $\mathbf{Y}$  arrays. This method was further elaborated and lastly improved with respect to residual analyses by introducing a core array in the model of  $\mathbf{X}$  [2].

Considering an  $\mathbf{X}$  array of dimension  $I \times J \times K$ , the NPLS model is obtained by modeling  $\mathbf{X}$  as in Tucker3 decomposition:

$$\mathbf{X} = \mathbf{T}\mathbf{G}_x(\mathbf{W}^k \otimes \mathbf{W}^j)^T + \mathbf{E}_x \quad (1)$$

where  $\mathbf{X}$  is the  $\mathbf{X}$  array unfolded to an  $I \times JK$  matrix,  $\mathbf{T}$  holds the first mode scores (sample mode),  $\mathbf{W}^j$  and  $\mathbf{W}^k$  are the second and the third mode weights, respectively. The symbol  $\otimes$  denotes the Kronecker product [5].

$\mathbf{G}_x$  is the matricized core array of size  $F \times F \times F$  where  $F$  is the number of NPLS components (factors) and it is defined by:

$$\mathbf{G}_x = \mathbf{T}^+ \mathbf{X} ((\mathbf{W}^k)^+ \otimes (\mathbf{W}^j)^+)^T \quad (2)$$

Here the superscript '+' means that the Moore–Penrose is pseudo inverse.

In the case of a two-way data matrix,  $\mathbf{Y}_{I,M}$  is defined by: 146

$$\mathbf{Y} = \mathbf{U}\mathbf{Q} + \mathbf{E}_y \quad (3)$$

where  $\mathbf{U}$  holds the  $\mathbf{Y}$  scores and  $\mathbf{Q}$  is the loading matrix. 148

$\mathbf{E}_x$  and  $\mathbf{E}_y$  hold  $\mathbf{X}$  and  $\mathbf{Y}$  residuals, respectively. In analogy with the two-way PLS algorithm, the weights are determined such that the scores obtained from the  $\mathbf{X}$  decomposition ( $\mathbf{T}$ ) have maximum covariance with the scores obtained from  $\mathbf{Y}$  decomposition (inner relation:  $\mathbf{U} = \mathbf{T}\mathbf{B} + \mathbf{E}_y$ ). 149–153

By regressing the data onto their weights vectors, a score vector is found in the  $\mathbf{X}$ -space providing a least squares model of the  $\mathbf{X}$  data. Furthermore, by choosing the weights such that the covariance between  $\mathbf{X}$  and  $\mathbf{Y}$  is maximized a predictive model is obtained as: 154–157

$$\mathbf{Y} = \mathbf{T}\mathbf{B}\mathbf{Q} + \mathbf{E}_y \quad (4)$$

Regression coefficients that apply directly to  $\mathbf{X}(I \times JK)$  may also be derived [4,22]: 158–161

$$\mathbf{R} = \left[ w_1 (I - w_1 w_1^T) w_2 \dots \prod_{f=1}^{F-1} (I - w_f w_f^T) w_f \right] \quad (5)$$

$$\mathbf{B}_{\text{PLS}} = \mathbf{R}\mathbf{B} \quad (6)$$

$$\mathbf{Y} = \mathbf{X}\mathbf{B}_{\text{PLS}} \quad (7)$$

The NPLS-DA formulation is the same but the dependent variable block is a matrix  $\mathbf{Y}$  holding the class information, i.e. for each category a y-variable is defined as a dummy variable assuming values one/minus one to indicate class membership or not (notation one/zero is also used). As the predicted y-values can assume real values and not only minus one and one, classification of the samples is accomplished by assigning the sample to the category corresponding to the highest value of the predicted response, i.e. if the predicted vector of responses for an unknown sample, is:  $[-0.5 \ 0.8 \ 0.5]$  (in the case of three classes problem), it will be assigned to class two. 162–177

### 2.2. VIP calculation

#### 2.2.1. Two-way case

The variable importance in the projection (VIP) [17,19] represents the influence of each variable  $j$  of the data matrix  $\mathbf{X}_{I,J}$  on the model of the responses matrix  $\mathbf{Y}_{I,M}$  179–182

$$\text{VIP}_j^2 = S_j w_{jf}^2 \cdot \text{SSY}_f / J / (\text{SSY}_{\text{tot.expl.}} \cdot F) \quad (8)$$

where,  $F$  is the number of latent variables of the PLS model and  $J$  the number of  $\mathbf{X}$  variables. 183–185

In the case of mono-dimensional  $\mathbf{y}^{1 \times 1}$  holds: 186

$$\text{SSY}_f = b_{jf}^2 \mathbf{t}_f^T \mathbf{t}_f \quad \text{SSY}_{\text{tot.expl.}} = \mathbf{b}^2 \mathbf{T}^T \mathbf{T} \quad (9)$$

where  $\mathbf{T}$  is the  $\mathbf{X}$  score matrix and  $\mathbf{b}$  the PLS inner relation coefficients. 188

Thus a VIP value for each variable is computed in order to quantify its importance by using the PLS weight  $w_{jf}$  weighted by how much of  $\mathbf{y}$  is explained in each model dimension (latent variable). 189–191

VIP formulation as originally proposed [17] is intended to be a parameter varying in a fixed range since the sum of squared VIP for all variables is the sum to the number of variables. Thus, the variables with a VIP value larger than 1 (i.e. larger than the average of square VIP values) have an above average influence on the model and are, therefore, considered the most relevant for explaining  $\mathbf{Y}$ . The choice of the VIP threshold to assess the salient variables is a critical issue, as in any ranking method. The original proposal, that will be adopted here as well, of a threshold of one is acceptable if variable relevance is 192–200

discussed but feature selection is not accomplished. In the cases of marker identification and variable selection, resampling methods such as bootstrap are more appropriate [19,20] to assess the significance of the VIPs.

### 2.2.2. Three-way case

In the case of a two-dimensional  $\mathbf{Y}(I \times M)$  the previous relation applies to each mode, e.g. in the case of a three-way array  $\underline{\mathbf{X}}(I \times J \times K)$ :

$$\text{VIP}_j^2 = \sum_f w_{jf}^2 \cdot \text{SSY}_{mf} \cdot J / (\text{SSY}_{\text{tot.expl.m}} \cdot F) \quad (10)$$

$$\text{VIP}_k^2 = \sum_f w_{kf}^2 \cdot \text{SSY}_{mf} \cdot K / (\text{SSY}_{\text{tot.expl.m}} \cdot F) \quad (11)$$

where,  $F$  is the number of total latent variables,  $J$  the number of  $\mathbf{X}$  variables in Mode2 and  $K$  the number of variables in Mode3. For each latent variable  $f$ :

$$\text{SSY}_{\text{tot.expl.m}} = \sum_i (\mathbf{T}_{(I \times F)} \mathbf{B}_{(F \times F)} \mathbf{Q}_{(m,F)}^T)^2 \quad (12)$$

and each  $y$ -variable  $y_m$ :

$$\text{SSY}_{mf} = \sum_i (\mathbf{t}_f b_{fj} q_{m,f})^2 \quad (13)$$

where,  $I$  is the number of samples in Mode2,  $\mathbf{T}$  is the Mode1 score matrix,  $\mathbf{B}$  holds the NPLS inner relation coefficients and  $\mathbf{Q}$  the  $\mathbf{Y}$  loadings.

For a given model dimension  $f$  and each variable  $j$ , the VIP value is given by the squared weight  $w_{jf}^2$  of that parameter (i.e. the weight  $w_{jf}$  indicates the importance of the  $j$ th variable in the model dimension  $f$ ), multiplied by the percent of  $\mathbf{Y}$  explained sum of squares by that  $f$  dimension.

The variable importance is then normalized so that  $\text{VIP}^2$  equals the number of the variables.

While considering all  $\mathbf{Y}$  variables together, Eqs. (12) and (13) are reduced to:

$$\text{SSY}_{\text{tot.expl.}} = \sum_i (\mathbf{T}_{(I \times F)} \mathbf{B}_{(F \times F)} \mathbf{Q}_{(M,F)}^T)^2 \quad (14)$$

$$\text{SSY}_f = \sum_m \sum_i (\mathbf{t}_f b_{fj} \mathbf{q}_{m,f}^T)^2 \quad (15)$$

and Eq. (10) is reduced to: 230

$$\text{VIP}_j^2 = \sum_f w_{jf}^2 \cdot \text{SSY}_f \cdot J / (\text{SSY}_{\text{tot.expl.}} \cdot F). \quad (16)$$

Extension to the other  $\mathbf{Y}$  modes can be easily obtained. 233

### 3. Data sets and pretreatment 234

In this study, we present applications of VIP to different three-way data sets. Two data sets are related to optimization of food processing and authentication issue for products with protected denomination of origin, respectively, and the third one is related to a neuroscience problem. Each data set allows exploring the different situations, predictive and discriminant models, partial and overall VIP contribution with respect to  $\mathbf{Y}$  block together with the different aspects of complementary information that VIP can highlight with respect to e.g. NPLS weights or regression coefficients. 243

#### 3.1. Data set 1: Bread 244

Li Vigni and Cocchi [24] presented a multi-way study related to the influence of flour formulation on bread quality. Ten different flour mixtures were investigated by means of Near Infrared Spectroscopy (NIRS) to obtain information on flour performance in a critical phase such as dough leavening. For each mixture, a laboratory-scale bread making experiment was carried out according to a standardized recipe and the leavening phase of each dough sample was monitored by means of NIRS at different times. NPLS was applied to model the properties of bread loaves (dimensions, volume, weight, height) from near infrared spectra, acquired at different leavening times, of the dough obtained from different flour formulations. 255

The data are arranged as follows and schematically shown in Fig. 1: 256

-  $X$ -block: a three-way array  $\underline{\mathbf{X}}(I \times J \times K)$  (10 flour mixtures  $\times$  173 NIR wavelengths  $\times$  7 leavening time intervals) 258

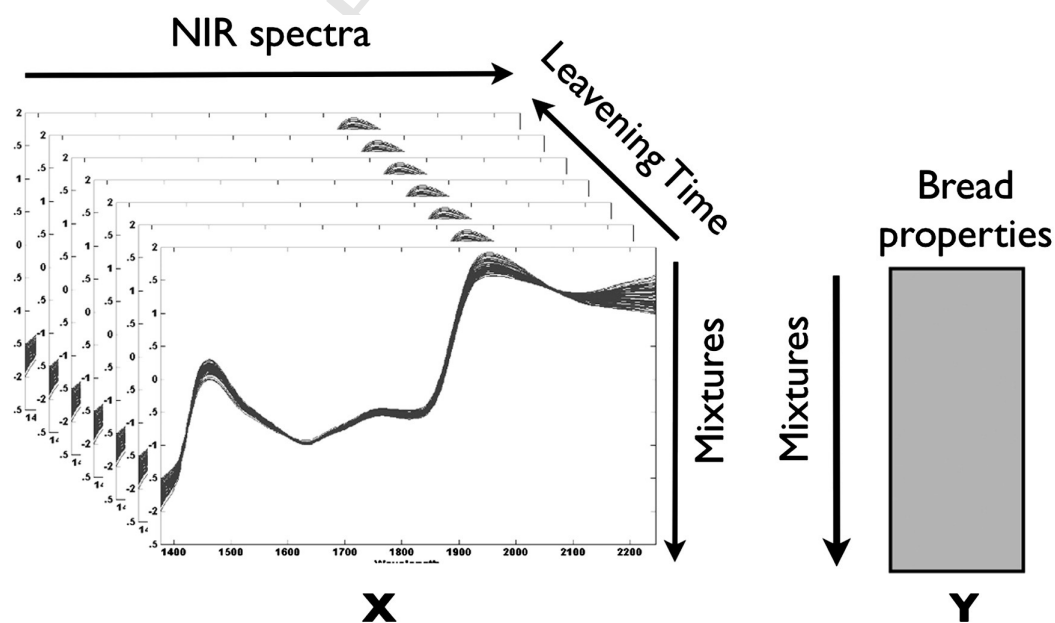


Fig. 1. Data set arrangement for Bread data. (Left) NIR data ( $\mathbf{X}$ ): Mode1, samples (the 10 different mixtures); Mode2, NIR spectra (173 wavelengths); Mode3, leavening time points (7). (Right) Bread property data ( $\mathbf{Y}$ ): Mode1, samples (the 10 different mixtures); Mode2, bread properties (4).

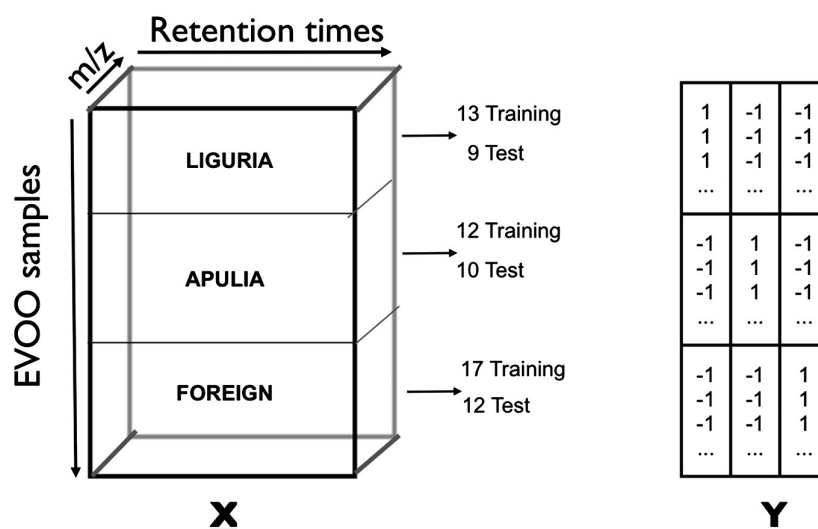


Fig. 2. Data set arrangement for EVOO data. (Left) GC–MS data ( $\mathbf{X}$ ): Mode1, samples; Mode2, Retention times (1514 time points); Mode3, 77 selected m/z fragments. (Right) Dummy class variables ( $\mathbf{Y}$ ): Mode1, samples; Mode2 classes (3).

259 -  $Y$ -block:  $\mathbf{Y}(I \times M)$  (10 flour mixtures  $\times$  4 bread loaf properties:  
260 weight, height, diameter and density).

261 NIR signals were preprocessed by applying Savitsky–Golay Smooth-  
262 ing (15 points window, second order polynomial) coupled to Standard  
263 Normal Variate normalization (SNV) to remove the baseline shift.

264 VIP values are used to assess the spectral regions mainly involved  
265 in determining flour performance.

### 266 3.2. Data set 2: Extra virgin olive oil (EVOO)

267 The data set [25] consists of a set of extra virgin olive oil (EVOO), be-  
268 longing to different olive cultivars and coming from different Mediter-  
269 ranean areas: Liguria (Northern Italy), Apulia (Southern Italy), Greece,  
270 Tunisia and Spain. The aim is to assess the authenticity of Ligurian  
271 EVOO that has been designed by protected denomination of origin  
272 (PDO) certification and represents one of the most highly esteemed  
273 EVOOs, of high economic value. The EVOO samples have been charac-  
274 terized by the analysis of aroma (Head Space Solid Phase Micro Extrac-  
275 tion coupled with Gas Chromatography–Mass Spectrometry, i.e.  
276 HS-SPME/GC–MS), which is well suited for analyzing the volatile  
277 fraction that is of relevance for the sensory quality of olive oil. The  
278 differentiation among classes has been obtained by NPLS-DA, defining  
279 three classes: Liguria, Apulia and Foreign, which includes the EVOO  
280 from Turkey, Spain and Greece.

281 The data set is arranged as follows (Fig. 2):

282 -  $X$ -block: a three-way array  $\mathbf{X}(I \times J \times K)$  (73 EVOO samples  $\times$  1514  
283 retention time points  $\times$  77 m/z fragments)

284 -  $Y$ -block:  $\mathbf{Y}(I \times M)$  (73 EVOO samples  $\times$  3 dummy variables hold-  
285 ing class memberships).

286 For each class the data were randomly split in a training and validation  
287 (test) set as shown in Fig. 2. The training set was preprocessed by center-  
288 ing across the first mode, block-scaling within the second mode, by defin-  
289 ing four retention time regions in order to allow both major and minor  
290 constituents to contribute to the model without up-weighting baseline  
291 contribution [25] and scaled by inverse standard deviation within the  
292 third mode (selected mass fragments). The pretreatments were applied  
293 in the order Mode3, Mode2, and Mode1.

294 VIP values were used to assess both GC and MS discriminant  
295 features.

### 3.3. Data set 3: Neuroscience data set

296

297 This data set derives from a functional magnetic resonance imag-  
298 ing (fMRI) experiment where the psychophysical pain profile, corre-  
299 sponding to subjective responses to acute prolonged noxious  
300 stimulation of one hand, was acquired in healthy volunteers. The ex-  
301 periment lasted 20 min (300 time points), the sensory intensity of  
302 pain (psychophysical pain profile) and the hemodynamic response  
303 (blood-oxygen-level contrast registered by a magnetic resonance  
304 pulse sequence, fMRI-BOLD signal) were recorded simultaneously  
305 during the experiment. The functional fMRI-BOLD signals (fMRI-BOLD  
306 time series) acquired at each brain voxel, as described in Prato et al.  
307 [26], were summarized for forty four brain regions of interest (ROIs)  
308 by taking the first principal singular vector (1st-SVD) of the data ma-  
309 trix containing the fMRI-BOLD time series for each voxel in that spe-  
310 cific ROI.

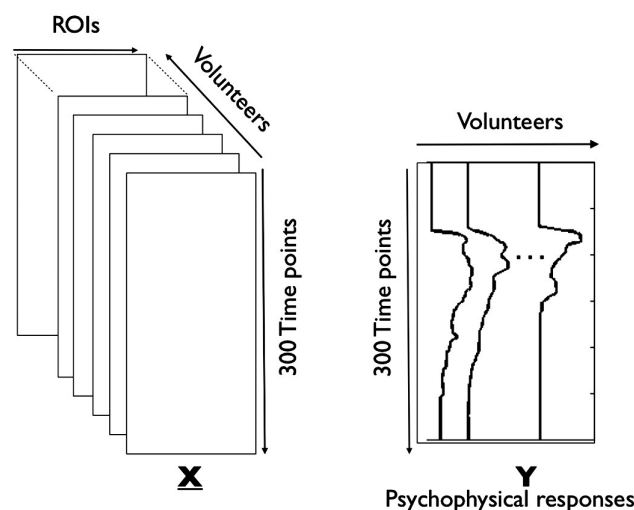


Fig. 3. Data set arrangement for Neuroscience data. (Left) fMRI-BOLD data ( $\mathbf{X}$ ): Mode1, Times Points (300); Mode2, fMRI-BOLD intensity for the 44 ROIs; Mode3, volunteers (10). (Right) psychophysical responses ( $\mathbf{Y}$ ): Mode1, Time points (300); Mode2, perceived pain intensity by volunteers (10), in this case the actual  $\mathbf{Y}(300 \times 1 \times 10)$  has been rotated for illustration purposes.



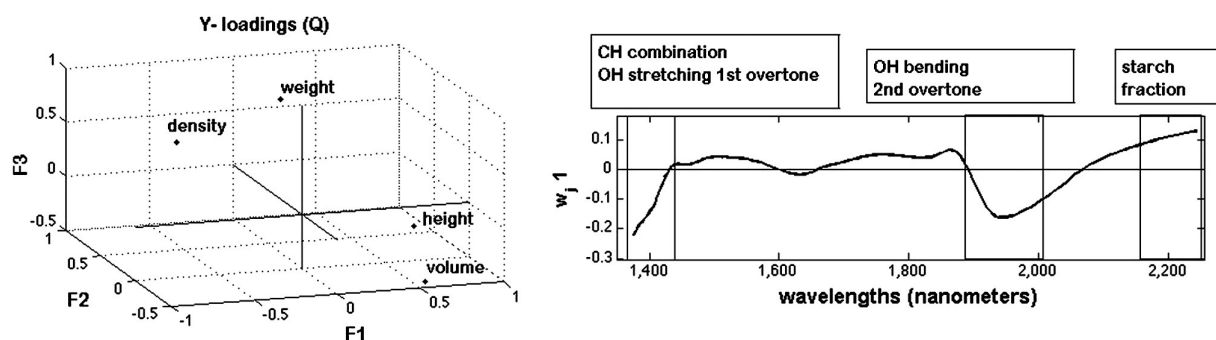


Fig. 4. Data set for Bread. (Left) Y-loadings plot (Q) for the three NPLS components, F1, F2, and F3; (Right) NPLS-weight plot for Mode2 (spectra), F1 vs. wavelengths.

NPLS was applied to build a model that could express the main variation of the ROI time series of different volunteers and obtain a fitted model that could reproduce the corresponding psychophysical pain profile efficiently.

The data arrays have been arranged as (Fig. 3):

- X-block: a three-way array  $\underline{X}(I \times J \times K)$  (300 time points  $\times$  44 ROIs  $\times$  10 volunteers).
- Y-block: the  $\underline{Y}(I \times 1 \times K)$  array is actually a matrix  $\underline{Y}(I \times K)$  comprised of 300 time points (psychophysical pain profile)  $\times$  10 volunteers, as shown in Fig. 3, and so computationally handled as such.

The choice of defining time as mode one was motivated by the applicability of the model. In fact, for this approach the main scope was to identify those ROI time series strictly connected (i.e., in terms of covariance) with the psychophysical pain profile of each volunteer (see Fig. 3).

The  $\underline{X}$  and  $\underline{Y}$  data were not centered or scaled within any mode.

VIP values were used for ranking the ROIs according to their relevance in the NPLS model hence to depict brain region activation profile in response to pain stimulus.

## 4. Results and discussion

### 4.1. Bread

Near infrared spectra acquired on dough at subsequent leavening times is an efficient way to characterize the leavening process. In particular, NPLS was used to study the relationship between the modifications recorded by the NIR signal during the leavening time and four properties measured on bread loaves, namely height, weight, volume and density. The dough samples correspond to ten different wheat mixtures (combining four distinct wheat varieties), performed according to a G-optimal design, thus bread performance can be linked to best mixture formulation in terms of wheat varieties.

The dimensionality of NPLS model was chosen on the basis of the best compromise of the minimum values of RMSECV for the four properties, modeled as a single Y block. Leave One Out cross validation was chosen due to the limited number of samples, ten.

A three factor NPLS model explains 75% of the total Y variance in fit, with acceptable performances in fit for all responses and generally poor results in cross-validation. As discussed in Ref. [24] these are mainly due to two mixtures showing extreme behavior in property space. However, a qualitative identification of the relationship among NIR signal variability along with the progression of the leavening step and bread properties can be obtained by inspecting NPLS model results.

In particular, Y loading plot (Fig. 4, left plot) shows that the first NPLS latent variable (F1) mainly models bread loaf height and volume, while latent variables 2 and 3 (F2 and F3) model bread loaf weight. NPLS Mode2 weights indicate which spectral regions mostly influence each factor and hence bread loaf properties. For example, the first factor for Mode2 weights ( $w_{j1}$ , Fig. 4, right plot), which is linked to height/volume

properties, shows that the most relevant contributions can be assigned to water and its redistribution across the macro-polymeric components of the dough, such as gluten and starch. In fact, the most relevant frequencies are those near 1400, and between 1900 and 1950 nm, for which weights have a negative sign, and above 2100 nm, for which weights have positive sign. These regions correspond, respectively, to absorptions that can be associated to the O–H stretching first overtone, the O–H bending second overtone mode and to overtone and combination mode contributions from the starch, protein and lipid fractions.

Inspection of Mode3 weights (leavening times, Fig. 5) indicates that height and volume are influenced by initial ( $t_0$ – $t_{10}$ ) and last leavening phases (yeast activity, dough strength); in fact these times have relevant weight values on the first NPLS factor (Fig. 5, top plot); weight is mainly influenced by initial ( $t_0$ ) time; hence flour properties are mostly important, as shown by second and third NPLS factor weights (Fig. 5, middle and bottom plots).

The regression coefficient maps are not so easily interpretable, see Fig. 6, while in order to assess the most relevant spectral regions and leavening times VIP values, proved to be very useful (Fig. 7A and B). Fig. 7A reports the VIP values for Mode3. It is interesting to notice that, for bread weight, the spectrum at the beginning of the leavening phase (time 0) has VIP values higher than one while height property exhibits significant alternating variation at times 10, 40 and 60. The other two properties, volume and density, show that the times at which the most significant variations in the NIR spectrum are recorded correspond mainly to the initial conditions (0 and 10 min) and the final one (60 min).

The most influential NIR spectrum regions, as highlighted by Mode2 VIP values (Fig. 7B), are the same for all properties: at about 1425 nm.

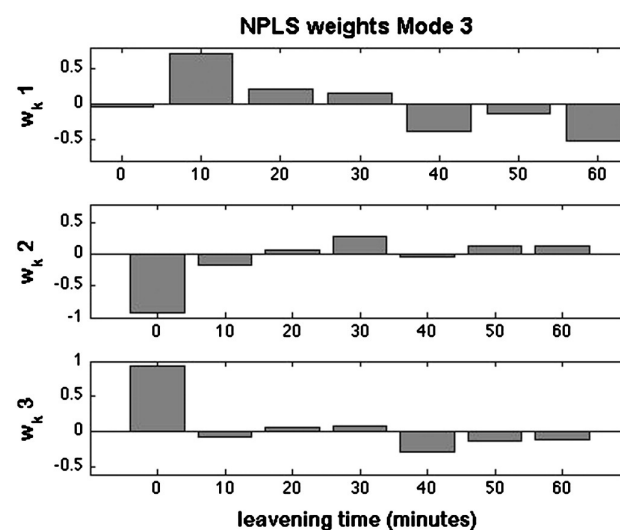


Fig. 5. Data set for Bread. Plot of NPLS weight for Mode3 (leavening times).

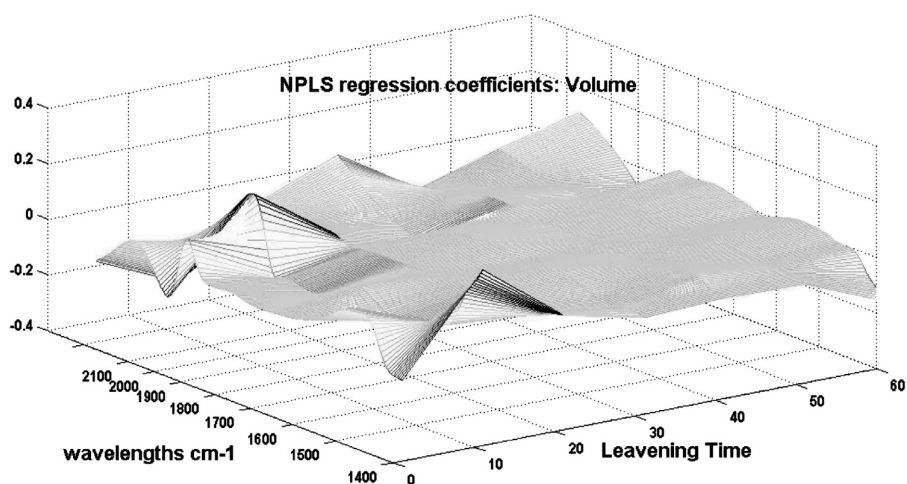


Fig. 6. Data set for Bread. 2D plot of the NPLS regression coefficient map for the y-property Volume.

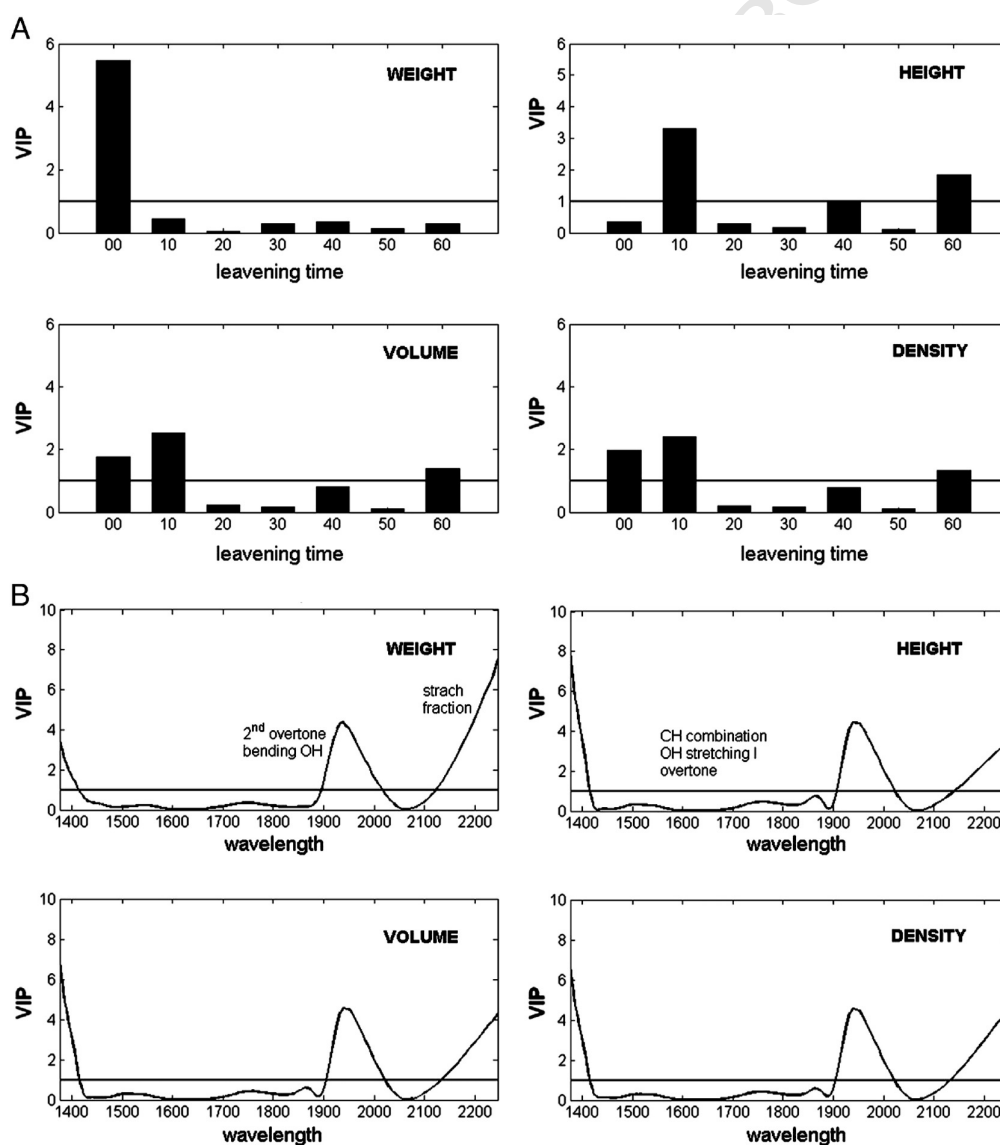


Fig. 7. Data set Bread. (A) Squared VIP values for Mode3 for each bread property; (B) squared VIP values for Mode2 for each bread property.

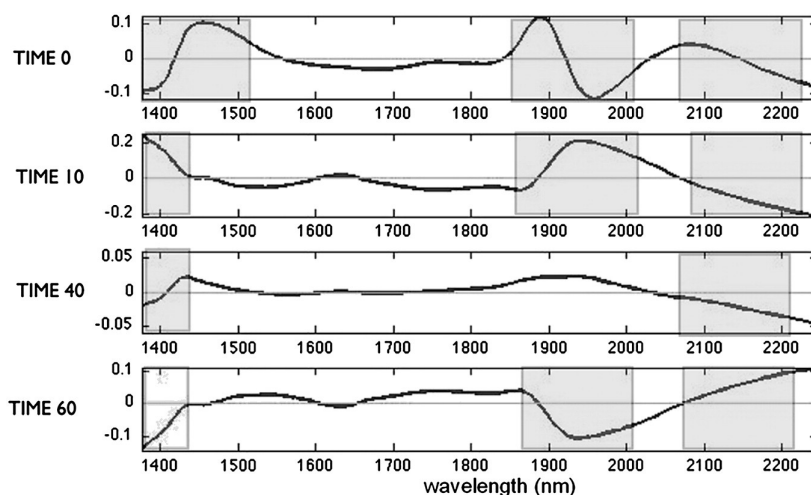


Fig. 8. Data set for Bread. Plot of NPLS regression coefficients at selected leavening times. Gray bar highlights the most relevant NIR spectral regions.

386 There are also contributions from C–H combination and first O–H  
 387 stretching overtone, between 1900 and 1950 nm, corresponding to  
 388 absorptions which can be associated to the second overtone O–H bending  
 389 mode, and above 2100 nm, where overtone and combination mode  
 390 contributions from the starch fractions are present.

391 On the basis of VIP analysis it is now possible to plot for each  
 392 modeled bread property the NPLS regression coefficients corresponding  
 393 only to the most influential leavening times, so that the spectral contribu-  
 394 tions can be discussed in terms of increasing/decreasing of specific  
 395 absorption bands, taking into account the regression coefficients sign,  
 396 in an easier way. Fig. 8, as an example, shows the regression coefficient  
 397 plot for the most relevant leavening times for the bread Volume. The  
 398 most significant spectral regions discussed above change correlation  
 399 sign at the different times as it may be expected by the dynamic of the  
 400 leavening process where several rearrangements of the starch and glu-  
 401 ten networks take place [24].

402 The combination of multi-way methods applied to NIR spectra is  
 403 here useful to supervise changes of the system according to the

404 leavening time, and can be used as a reference to evaluate the behav-  
 405 ior of dough obtained from different wheat flour mixtures, and poten-  
 406 tially to identify anomalous leavening situations. Also, it has been  
 407 shown that VIP values give the same information as the joint discus-  
 408 sion of Y loadings and NPLS weights, but with a more direct highlight  
 409 of the most influential contribution for each property. Moreover, they  
 410 can be taken into account as a guide to plot in an interpretable man-  
 411 ner the NPLS regression coefficients, which may otherwise result of  
 412 difficult interpretation.

#### 4.2. Extra virgin olive oil (EVOO)

413  
 414 The performance of the NPLS-DA classification models has been  
 415 evaluated by means of percentage of correct classification in cross-  
 416 validation (CV), by using venetian blind with six cancellation groups.  
 417 Three NPLS components gave the best performance with 100% correct  
 418 classification in fit and CV for Liguria and Foreign classes and 92% (fit  
 419 and CV) for Apulia. The test set for Liguria and Foreign classes was

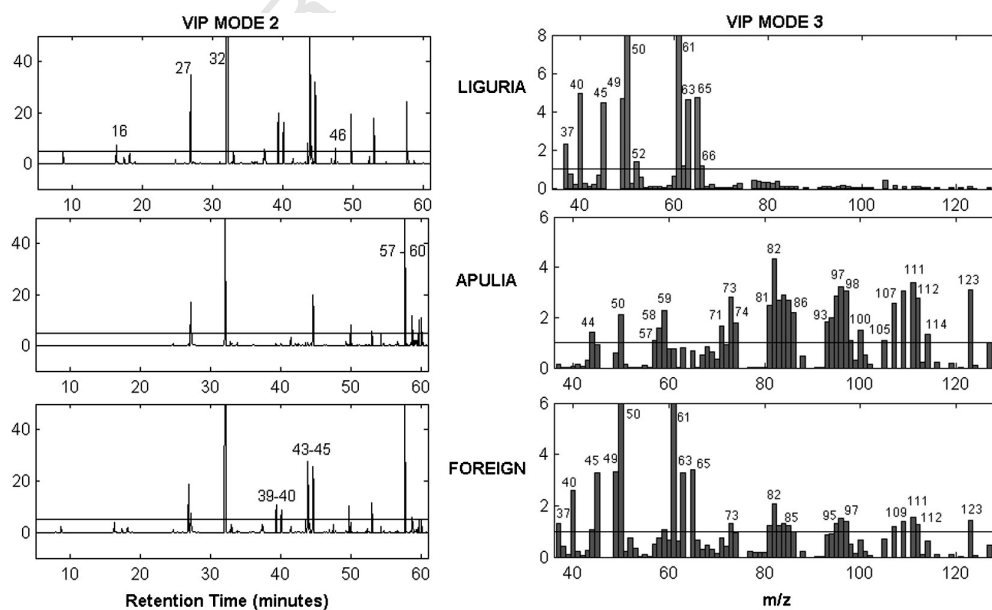


Fig. 9. Data set for EVOO. Plot of the squared VIP. (Left) Mode2 VIPs vs. Retention Times, threshold sets to 5. (Right) Mode3 VIPs vs. m/z fragments, threshold sets to 1.



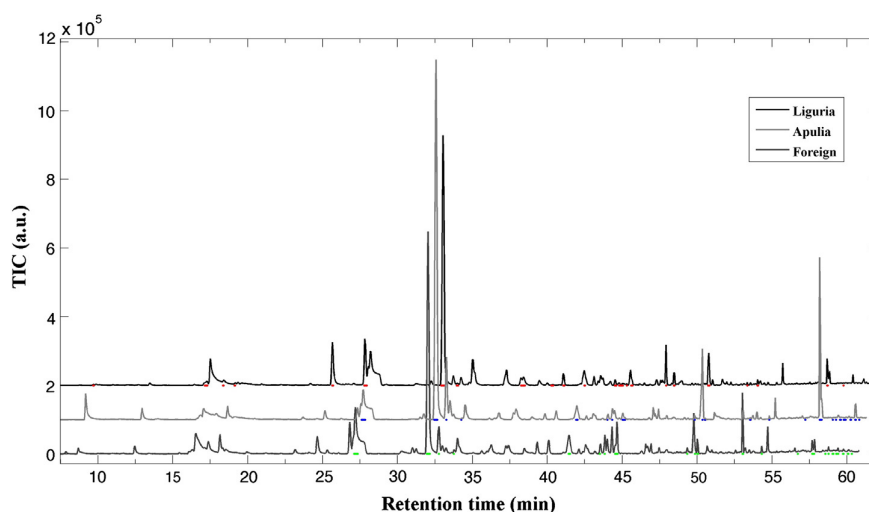


Fig. 10. Data set for EVOO. Average TIC chromatograms for each class, overlaid with a shift of 0.5 on time axis (x-axis) and of 1 on y-axis. Dots indicate retention time with VIP values higher than one.

420 correctly classified with no error and with one misclassified sample for  
421 Apulia.

422 The VIP values for Mode2 and Mode3 for each y-variable, hence category,  
423 are reported in Fig. 9. The VIP values threshold is drawn at 1 for  
424 Mode3 (m/z fragment), Fig. 9 on the right; while for Mode2 (Retention  
425 time) is drawn at 5, Fig. 9 on the left. This choice is motivated by consid-  
426 ering that this is the number of points generally defining a peak, thus a  
427 variable to be considered important has to have a contribution at least  
428 as one peak in the signal. Taking into account the most important vari-  
429 ables of both modes some considerations about the main compositional  
430 difference of each EVOO category can be made. The chromatographic  
431 peaks, which seem to characterize the volatile fraction of Liguria olive  
432 oil, are some low molecular weight compounds (Retention time about  
433 16 min;  $m/z < 40$ ) and C6 linear unsaturated aldehydes (Retention  
434 time regions at about 27 min and 32 min;  $m/z$  region 61–70) character-  
435 istics of high quality virgin olive oils. The latter compounds are also

present in Apulia and the Foreign class but in a lower amount. The Apu- 436  
lia class is mainly characterized by the retention time region 57–60 437  
and by higher molecular weights compounds ( $m/z$  values higher than 438  
80), such as alpha-copaene ( $Rt = 57.7$  min;  $m/z$  81, 93, 105). The 439  
high VIP values (mainly for Liguria and Foreign classes) at the retention 440  
time regions 39–40 and 43–45 min highlight compounds that are more 441  
related to, i.e. specific for, the Foreign class as it can be seen from Fig. 10, 442  
where the average total ion count chromatograms (TIC) for each class 443  
are shown. 444

The NPLS weights for Mode2 and Mode3 for each of the three NPLS 445  
components (F1, F2 and F3) are reported in Fig. 11. In order to interpret 446  
these plots the Y loadings have to be inspected (figure not shown). These 447  
indicate that Liguria (y1) has high positive loadings on components 2 448  
and 3 (F2 and F3) and close to zero on component 1 (F1), the opposite 449  
holds for Foreign (y3) while Apulia has high positive loadings values 450  
on component 1 (F1) and almost zero on the other two components. 451

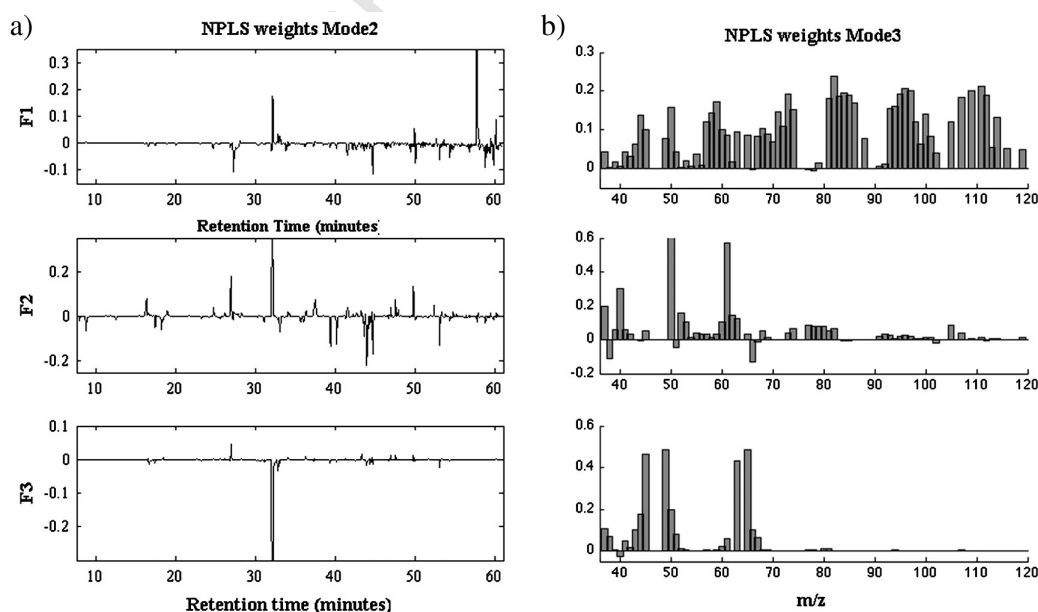
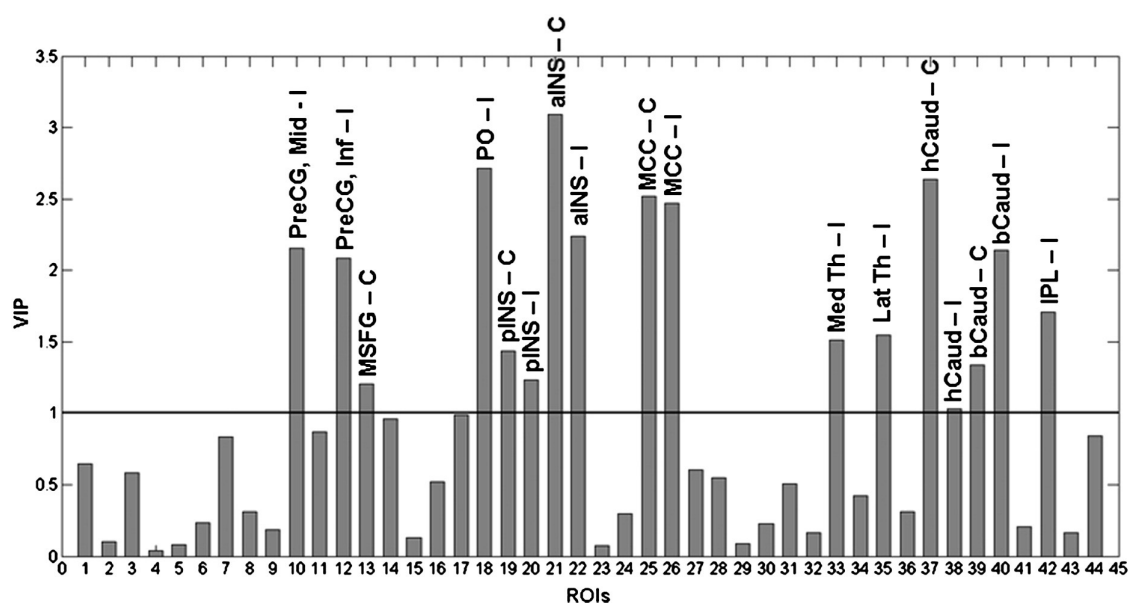


Fig. 11. Data set EVOO. (a) NPLS weights for Mode2 vs. retention times, for NPLS components F1 (top), F2 (middle) and F3 (bottom). (b) NPLS weights for Mode3 vs.  $m/z$  fragments, for NPLS components F1 (top), F2 (middle) and F3 (bottom).



**Fig. 12.** Data set for Neuroscience. Plot of the squared VIP calculated for all  $\mathbf{Y}$  altogether vs. ROIs, the threshold is set to 1. Labels refer to ROIs: Contralateral (C) and Ipsilateral (I) to the injected hand, respectively; Pre-Central Gyrus (PreCG), Middle (Mid); Medial Superior Frontal Gyrus/Paracentral Lobule (MSFG); Parietal Operculum (PO); Posterior Insula (pINS); Anterior Insula (aIns); Mid-Cingulate Cortex (MCC); Medial Thalamus (Med Th); Lateral Thalamus (Lat Th); Caudate Nucleus, head (hCaud); Caudate Nucleus, body (bCaud); Inferior Parietal lobule (IPL).

452 Taking this into account by looking at the Mode2 weights (Fig. 11a) the  
 453 observations about the characteristics retention time regions for each  
 454 class, made on the basis of the VIP values, are confirmed, e.g. the negative  
 455 sign of the weights at retention time 39–40 and 43–45 indicates that this  
 456 region is characteristic of the Foreign class.

#### 457 4.3. Neuroscience data set

458 The goal was to build a model that, starting from the fMRI-BOLD  
 459 characterization as expressed by the 1st SVD component of each ROIs  
 460 fMRI-BOLD time series, could predict efficiently the psychophysical  
 461 pain intensity for each volunteer. A NPLS model with 4 Latent Variables  
 462 (LVs) was selected according to Cross Validation results, lowest  
 463 RMSECV value, i.e. 28.12, with explained  $\mathbf{Y}$  variance around 95%.

The VIP values were used for ranking the brain regions (ROIs) main- 464  
 ly involved in pain perception. In this case it is interesting to consider 465  
 the VIP values calculated for the overall  $\mathbf{Y}$ -responses, to gain a global 466  
 picture of brain activation common to all subjects. Fig. 12 reports the 467  
 VIP values versus ROI number as bar plot, highlighting the ROIs showing 468  
 VIP values greater than one. These brain regions are in agreement with 469  
 the results reported in Prato et al. [26]. 470

The information gathered by the VIPs is complementary to the one 471  
 carried by the N-PLS weights. Fig. 13 reports the weights for the first 472  
 two N-PLS factors for the second mode (ROIs). Extreme positive  $\mathbf{w}_j$  473  
 values on F1 are those related to ROI with VIP values higher than 474  
 one. Inspection of the corresponding weights plot for Mode3 (volun- 475  
 teers), i.e.  $\mathbf{w}_k$ , Fig. 14, shows that the different volunteers are distribu- 476  
 ted along the first factor that differentiates e.g. volunteer #9 from 477  
 volunteer #10. 478

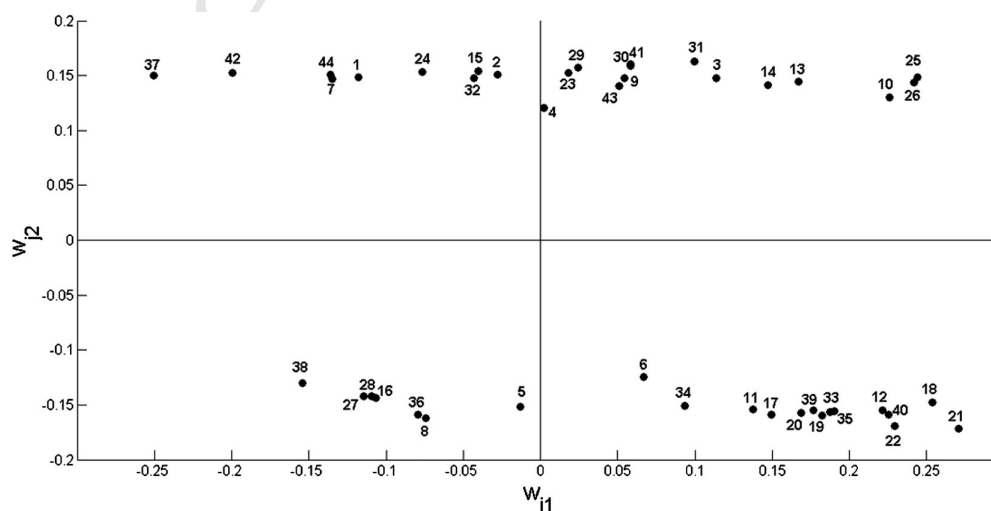


**Fig. 13.** Data set for Neuroscience. Scatter plot of NPLS weights for Mode2 (ROIs): first vs. second component.

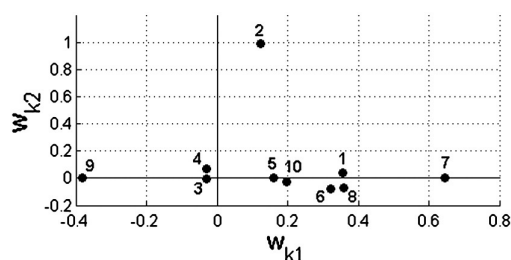


Fig. 14. Data set for Neuroscience. Scatter plot of NPLS weights for Mode3 (volunteers): first vs. second component.

479 This can be discussed by considering the different behaviors in perceived pain as underlined by the first mode loadings plots (functional fMRI profiles), shown in Fig. 15. The first factor describes the average pain profile, the second seems almost dedicated to a delayed maximum peak and more persistent pain. High positive loading values on factor one for Mode2, Fig. 14 (see for instance volunteer #7) represent an opposite behavior with an anticipated maximum peak in comparison with the average pain profile. The highest negative value (volunteer #9) with the extreme negative position (with respect to the abscissa) identifies a positive shift of the maximum pain perceived in comparison with the mean profile (reference volunteer #3). This may be retrieved by direct observation of the psychophysical responses for these subjects in comparison with those subjects showing a profile close to average as subjects three, see Fig. 16.

493 The second factor can be considered as a component that takes into account a sort of “prolonged activation due to tonic pain input” (see Fig. 15, in gray dashed) and it is particularly dedicated to describe volunteer #2 with its ample bell-shape of the pain perceived. In Fig. 16 the comparison between the pain profiles of volunteer #2 and the reference volunteer #3 is shown. High weight  $w_{k2}$  value (see Fig. 14) for this volunteer seems to be only related to its particular behavior that is also responsible for the separation of the ROI regions in two groups with respect to the weight values on the second mode (Fig. 13).

502 Thus, discussion of the weights plot is useful to recover the detailed information on specific subject behavior while the overall VIP values point to the most relevant ROIs whose activation is involved in pain perception and that are thus capable of reproducing the Y-psycho responses.

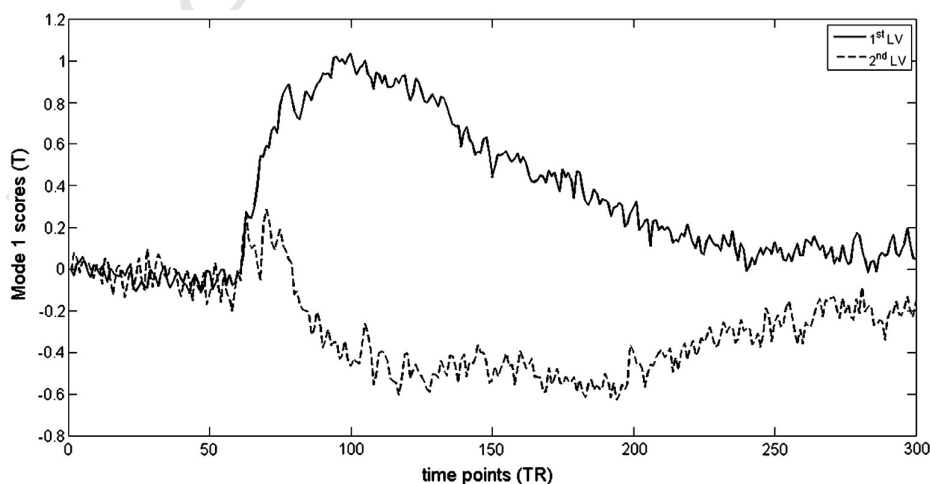


Fig. 15. Data set for Neuroscience. Mode1 loading (score) plot vs. time points (the temporal mode showing the evolution of functional fMRI-BOLD): (black) first component; (gray dashed) second component.

## 5. Conclusions

507

508 The recent developments in feature selection methods for two-way data have addressed the problem of increasing the performance of regression models, such as PLS. Complex filter, wrapper or embedded methods [11,20] improve predictor performance compared to simpler variable ranking methods, but the improvements are not always significant, they are computationally costly and in case of a large number of variables, the risk of over-fitting can be not negligible in the process of variable selection. The extension of variable selection methods to the multi-way data arrays, in multilinear regression context (NPLS, NPLS-DA) without recurring to unfolding, has been rather limited.

518 In this work, we introduced an extension of the Variable Importance in Projection (VIP) parameter to multi-way arrays. The proposed method has been tested on three different data sets where VIPs were discussed comparatively with respect to NPLS weight and regression coefficients.

522 VIPs naturally point out the identification of the most relevant variables related to  $Y$  in a multi-way array  $X$ . In particular, VIPs can be calculated for each mode of  $X$  and both considering the single  $y$ -responses or all the  $Y$  altogether. The former can be useful to assess the relevant variables with respect to each modeled properties, especially in the case of discriminant NPLS-DA to highlight the discriminant features, since each  $y$ -variable corresponds to a given class. While the latter offer a useful summary in order to operate feature selection.

530 However, when considering VIP, it is important to remember that, from an interpretative point of view, this metric suffers from the fact that PLS/NPLS components carry with them the unresolved contribution of both  $Y$ -related and  $Y$ -orthogonal parts of the  $X$ -variance. Both contributions are fundamental for a correct prediction of  $Y$  and the VIP metric represents a valid support whenever the interest is aimed to rank variables according to their influence to the whole model, while for contexts and purposes where the interest is mainly focused on assessing the  $X$ -part covarying with  $Y$  only, other methodologies may represent a valuable solution, such as OPLS [28] and Selectivity Ratio metric [21].

540 In the studied cases, VIPs provided an easier and complementary way to interpret the variable relevance in NPLS models, especially when examination of regression coefficients was not so straightforward due to the unreadable complex patterns associated [27], as in the case of spectral data (as for the Bread data set) and moreover with two signal dimensions as in the case of hyphenated analytical techniques. In the EVOO application, which is an example of chromatography/mass spectrometry data, the joint information from the VIPs on the retention time and  $m/z$  directions allows discussion in chemical terms of the most discriminant features.

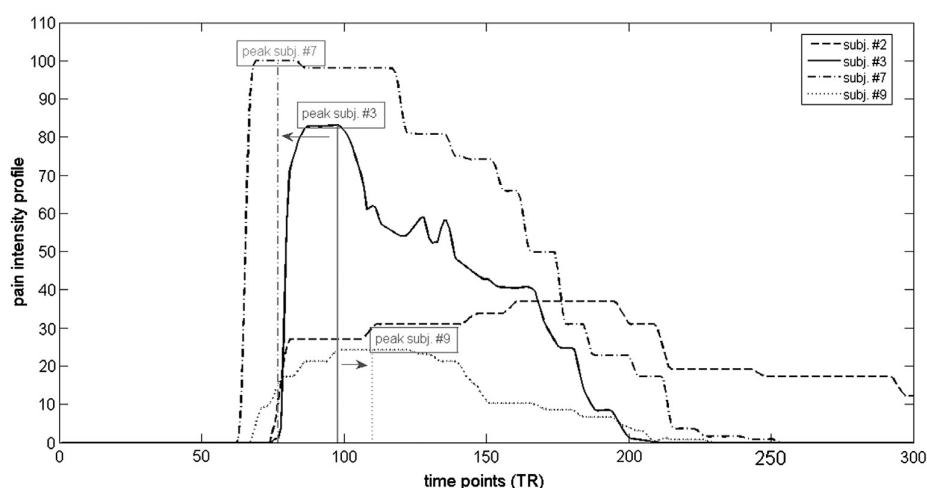


Fig. 16. Data set for Neuroscience. Pain intensity profile (psychophysical response) vs. time points, for some reference volunteers: subject #3 (solid black), subject #2 (dashed), subject #7 (dot-dashed) and subject #9 (dotted).

550 NPLS weights carry the information about the relevance of variables  
551 and sign of correlation with the modeled responses. However, they re-  
552 quire to be discussed together with the Y loadings and per component.  
553 In this respect, the VIPs are complementary pointing to the most influ-  
554 ential variables for each property on taking into account all components  
555 but of course require inspection of weights to assess the direction of the  
556 effect (increasing or decreasing the response values). Finally, the results  
557 obtained on the Neuroscience dataset were found to be in line with  
558 those published with a completely different method belonging to the  
559 machine learning field [26] as far as ranking of the most influential  
560 ROIs is concerned, while the use of multi-way models added the possi-  
561 bility to discuss both the common pattern to all volunteers in pain per-  
562 ception as well as the peculiar behavior of specific ones.

## Q10 563 6. Uncited reference

564 [23]

## 565 Acknowledgments

566 The “Functional Neuroimaging” group, of the Department of Bio-  
567 medical Sciences, Metabolic and Neuroscience, University of Modena  
568 and Reggio Emilia are kindly acknowledged for providing the fMRI  
569 data and for the support given in the discussion and interpretation  
570 of the results on this data set.

## 571 References

- Q11 572 [1] R. Bro, Multi-way calibration. Multi-linear PLS, *Journal of Chemometrics* 10 (1996)  
573 47–61.  
574 [2] R. Bro, A.K. Smilde, S. De Jong, On the difference between low-rank and subspace  
575 approximation: improved model for multi-linear PLS regression, *Chemometrics*  
576 *and Intelligent Laboratory Systems* 58 (2001) 3–13.  
577 [3] A. Smilde, Comments on multilinear PLS, *Journal of Chemometrics* 11 (1997)  
578 367–377.  
579 [4] S. De Jong, Regression coefficients in multilinear PLS, *Journal of Chemometrics* 12  
580 (1998) 77–81.  
581 [5] A. Smilde, R. Bro, P. Geladi, Multi-way analysis with applications, *Multi-way Anal-*  
582 *ysis in the Chemical Sciences*, Chpt 3.1, John Wiley & Sons, 2004, pp. 35–45.  
583 [6] E. Salvatore, M. Bevilacqua, R. Bro, F. Marini, M. Cocchi, Classification methods for  
584 multi-way arrays as a basic tool for food PDO authentication, in: M. De La Guardia,  
585 A. Gonzalez Illueca (Eds.), *Food Protected Designation of Origin: Methodologies*  
586 *& Applications*, Wilson & Wilson's Comprehensive Analytical Chemistry, vol. 60,  
587 Elsevier B.V., 2013.  
588 [7] P. Nomikos, J.F. MacGregor, Multivariate SPC charts for monitoring batch process-  
589 es, *Technometrics* 37 (1995) 41–59.  
590 [8] C. Durante, M. Cocchi, M. Grandi, A. Marchetti, R. Bro, Application of N-PLS to gas  
591 chromatographic and sensory of traditional balsamic vinegars of Modena,  
592 *Chemometrics and Intelligent Laboratory Systems* 83 (2006) 54–65.  
593 [9] C.M. Rubingh, M.J. van Erk, S. Wopereis, T. van Vliet, E.R. Verheij, N.H.P. Chubben,  
594 B. van Ommen, J. van der Greef, H.F.J. Hendriks, A.K. Smilde, Discovery of subtle  
595 effects in a human intervention trial through multilevel modeling, *Chemometrics*  
596 *and Intelligent Laboratory Systems* 106 (2011) 108–114.  
597 [10] A. Conesa, J.M. Prats-Montalbán, S. Tarazona, M.J. Nueda, A. Ferrer, A multiway  
598 approach to data integration in systems biology based on Tucker3 and N-PLS,  
599 *Chemometrics and Intelligent Laboratory Systems* 104 (2010) 101–111.  
600 [11] T. Mehmood, K.H. Liland, L. Snipen, S. Sæbø, A review of variable selection  
601 methods in partial least squares regression, *Chemometrics and Intelligent Labo-*  
602 *ratory Systems* 118 (2012) 62–69.  
603 [12] L. Norgaard, A. Saudland, J. Wagner, J.P. Nielsen, L. Munck, S.B. Engelsen, Interval  
604 partial least squares regression (iPLS): a comparative chemometric study with an  
605 example from near-infrared spectroscopy, *Applied Spectroscopy* 54 (2000) 413–419.  
606 [13] R. Leardi, A.L. Gonzales, Genetic algorithms applied to feature selection in PLS re-  
607 gression: how to use them, *Chemometrics and Intelligent Laboratory Systems* 41  
608 (1998) 195–207.  
609 [14] L. Stordrange, T. Rajalahtia, F.O. Libnau, Multiway methods to explore and model  
610 NIR data from a batch process, *Chemometrics and Intelligent Laboratory Systems*  
611 70 (2004) 137–145.  
612 [15] P.J. Odman, C. Lindvald, L. Olsson, et al., Sensor combination and chemometric  
613 variable selection for online monitoring of *Streptomyces coelicolor* fed-batch culti-  
614 vations, *Applied Microbiology and Biotechnology* 86 (2010) 1745–1759.  
615 [16] G. Lorho, F. Westad, R. Bro, Generalized correlation loadings. Extending correla-  
616 tion loadings to congruence and to multi-way models, *Chemometrics and Intelli-*  
617 *gent Laboratory Systems* 84 (2006) 119–125.  
618 [17] S. Wold, E. Johansson, M. Cocchi, PLS: partial least squares projections to latent  
619 structures, in: Hugo Kubinyi (Ed.), *3D QSAR in Drug Design: Theory, Methods*  
620 *and Applications*, ESCOM Science Publishers, Leiden, ISBN: 90-72199-14-6,  
621 1993, pp. 523–550.  
622 [18] S. Wold, M. Sjöström, L. Eriksson, PLS-regression: a basic tool of chemometrics,  
623 *Chemometrics and Intelligent Laboratory Systems* 58 (2001) 109–130.  
624 [19] I.G. Chong, C.H. Jun, Performance of some variable selection methods when  
625 multicollinearity is present, *Chemometrics and Intelligent Laboratory Systems* 78  
626 (2005) 103–112.  
627 [20] R. Gosselin, D. Rodrigue, C. Duchesne, A bootstrap-VIP approach for selecting  
628 wavelength intervals in spectral imaging applications, *Chemometrics and Intelli-*  
629 *gent Laboratory Systems* 100 (2010) 12–21.  
630 [21] T. Rajalahti, R. Arneberg, F.S. Berven, K.M. Myhr, R.J. Ulvik, O.M. Kvalheim, Bio-  
631 marker discovery in mass spectral profiles by means of selectivity ratio plot,  
632 *Chemometrics and Intelligent Laboratory Systems* 95 (2009) 35–48.  
633 [22] E. Acar, C. Aykut-Bingol, H. Bingol, R. Bro, A.L. Ritaccio, B. Yener, Modeling and de-  
634 tection of epileptic seizures using multi-modal data construction and analysis,  
635 Technical Report, 2008, (Computer Science Department at RPI (<http://www.cs.rpi.edu/research/tr.html>)).  
636 [23] J. Nilsson, S. De Jong, A.K. Smilde, Multiway calibration in 3D QSAR, *Journal of*  
637 *Chemometrics* 11 (1997) 511.  
638 [24] M. Li Vigni, M. Cocchi, Near infrared spectroscopy and multivariate analysis to  
639 evaluate wheat flour doughs leavening and bread properties, *Analytica Chimica*  
640 *Acta* 764 (2013) 17–23.  
641 [25] C. Durante, R. Bro, M. Cocchi, A classification tool for N-way array based on SIMCA  
642 methodology, *Chemometrics and Intelligent Laboratory Systems* 106 (2011) 73–85.  
643 [26] M. Prato, S. Favilla, L. Zanni, C.A. Porro, P. Baraldi, A regularisation algorithm for  
644 decoding perceptual temporal profiles from fMRI data, *NeuroImage* 56-1 (2011)  
645 258–267.  
646 [27] A.J. Burnham, J.F. MacGregor, R. Viveros, Interpretation of regression coefficients under  
647 a latent variable regression model, *Journal of Chemometrics* 15 (2001) 265–284.  
648 [28] J. Trygg, S. Wold, *Journal of Chemometrics* 17 (2003) 53–64.  
649  
650